TASK QUARTERLY 4 No 3 (2000), 469–484

THE EVOLUTION OF STRAIN LOCALISATION IN A HYPOPLASTIC COSSERAT MATERIAL UNDER SHEARING

ERICH BAUER AND WENXIONG HUANG

Institute of General Mechanics, Graz University of Technology
Kopernikusgasse 24, A-8020 Graz, Austria
bauer@mech.tu-graz.ac.at
huang@mech.tu-graz.ac.at

(Received 26 March 2000)

Abstract: Numerical studies of the evolution of strain localisation and polar effects within a plane layer of a granular material under monotonic shearing are presented. Herein a micro-polar approach is formulated within the framework of a hypoplastic Cosserat continuum to describe the essential properties of a dry and cohesionless granular material like sand. The constitutive model is based on incremental non-linear tensor-valued functions and captures the influence of the pressure, the void ratio, the mean grain diameter and the rotation resistance of the grains on the evolution of the stresses and couple stresses. The Cosserat boundary conditions are suitable to model the rotation resistance at the interface between the granular layer and the surfaces adjoining the boundaries of the granular body. The numerical investigations show that the location, thickness and evolution of strain localisation within the shear layer are strongly influenced by the boundary conditions and the initial state quantities.

Keywords: localisation, granular material, polar effects, shearing, finite element method

1. Introduction

The concentration of shear deformations in narrow zones called shear bands is a well-known phenomenon found in granular materials. The location, orientation and thickness of a shear band are determined by the mechanical properties of the material and the boundary conditions. For large shearing dilatancy, strain softening and polar effects, *i.e.* pronounced grain rotations, can be observed (*e.g.* Bogdanova-

Bontcheva and Lippmann 1975, Oda 1993). The results of shear tests with sand specimens show that the thickness of the localised deformation zone is not a material constant. The thickness mainly depends upon the grain distribution, grain shape, stress level, initial density, dilatancy resistance of the boundaries and the roughness of the surfaces adjoining the boundaries of the granular body (*e.g.* Mühlhaus and Vardoulakis 1987, Gudehus 1993, Vardoulakis and Sulem 1995, Oda *et al.* 1996, Tejchman 1997, Uesugi *et al.* 1998). For an initially dense sand specimen the void ratios within the localised zone may increase beyond the critical value obtained from the standard test (Oda *et al.* 1997). It is worth noting that for numerical investigations an internal length must be included in the constitutive model. Otherwise the thickness of the localised zone in finite element calculations is scaled by the element size. As a result, the predicted load-displacement curves are unreliable in the post-bifurcation regime (*e.g.* de Borst *et al.* 1992). A polar continuum or so-called Cosserat continuum offers the possibility to include the mean grain diameter as an internal length in a physical natural manner (Mühlhaus 1986, Tejchman 1989). To this end a particular hypoplastic constitutive model according to Gudehus (1996) and Bauer (1996) based on the concept of a simple material was extended by quantities which are characteristic of a polar continuum (Bauer and Tejchman 1995, Tejchman and Bauer 1996, Tejchman 1997). The extended model takes into account Cosserat rotations, couple stresses, the mean grain diameter and the current void ratio which is related to the pressure-dependent maximum, minimum and critical void ratios. The constitutive equations for the stresses and couple stresses are incrementally non-linear tensor-valued functions which model anelastic behaviour. The model captures the influence of the pressure level and the current density on the incremental stiffness for both contractant or dilatant deformations using a single set of constitutive constants. All constitutive constants have a clear physical meaning and they can be determined from simple index and element tests (*e.g.* Herle and Gudehus 1999). Due to the presence of an internal length the boundary value problems are mathematically well-posed (de Borst *et al.* 1992) and the predicted thickness of the shear zone is not sensitive to the element size provided that the element size is small enough (Tejchman 1997). Based on this model numerical calculations were carried out for different boundary value problems involving the appearance of zones with localised deformations. The results show acceptable agreement with the experiments (*e.g.* Herle and Tejchman 1997, Wehr, Tejchman, Herle and Gudehus 1997). Further aspects referring to the capacity of the polar hypoplastic model have been outlined for instance by Gudehus (1997) and Tejchman and Gudehus (1999). In this paper a slightly modified version proposed by Bauer and Huang (1999) is used. In particular the stress limit condition is formulated as a function of the symmetric part of the stress deviator. Moreover, in the constitutive equation for the couple stresses the polar constant is placed in a similar way as the stress limit condition in the constitutive equation for the shear and normal stresses. For the finite element calculation a four-node element with a so-called selective reduced integration technique is used to alleviate volumetric locking.

The focus of the investigation is on studying the influence of the boundary conditions on the evolution of strain localisation and polar effects within a granular layer between two parallel plates under plane shearing. In contrast to a classical continuum the displacement-field across the shear layer is non-linear from the beginning of shearing even though the material is homogeneous in the initial state. Strain localisation may appear for large monotonic shearing either in the middle of the granular layer or close to one of the boundary plates. The location within the granular body is strongly influenced by the boundary conditions. Only with respect to the symmetry condition for an infinite shear layer the displacement field is independent of the co-ordinate in the direction of shearing. Otherwise the deformations become rather heterogeneous. The thickness of the localised zone is mainly determined by the mean grain diameter, the initial density, the pressure level and by the polar parameter which reflects the shape and surface roughness of the grains. If the localised zone occurs close to one of the bounding plates then the thickness is also influenced by the roughness of the plates, *i.e.* the interface behaviour is determined by the sliding and the rotation resistance of particles at the bounding surface. In this paper the interface behaviour is modelled with the Cosserat rotation prescribed at the boundaries of the granular layer. Herein an empirical formula proposed by Tejchman (1997) is used to relate the Cosserat rotations at the boundary to the surface roughness, the mean grain diameter and to the relative displacement. The numerical simulations show that for shearing under a constant vertical pressure the thickness of the localised zone is independent of the height of the layer, which is in accordance with the experimental observations.

2. Hypoplastic Cosserat model

In a Cosserat continuum a material point possesses displacement degrees of freedom u_i (i = 1, 2, 3) and rotational degrees of freedom which are called Cosserat rotations ω_i^c (i = 1, 2, 3). The gradient of the rotations $\partial \omega_i^c / \partial x_j$ corresponds to the curvatures κ_{ij} which are associated with the couple stresses μ_{ij}. As a consequence, the deformation tensor and the stress tensor are nonsymmetric. The rate of deformation D_{ij}^c and the rate of curvature $\dot{\kappa}_{ij}$ are defined as:

$$D_{ij}^c = D_{ij} + W_{ij} - W_{ij}^c, \quad \dot{\kappa}_{ij} = \partial \dot{\omega}_i^c / \partial x_j,$$

with

$$D_{ij} = \left[\partial \dot{u}_i / \partial x_j + \partial \dot{u}_j / \partial x_i \right] / 2 ,$$

$$W_{ij} = \left[\partial \dot{u}_i / \partial x_j - \partial \dot{u}_j / \partial x_i \right] / 2 ,$$

and

$$W_{ij}^c = -e_{kij} \dot{\omega}_k^c .$$

Herein $\dot{u}_i$ denotes the velocity, D_{ij} and W_{ij} are the symmetric and nonsymmetric parts of the velocity gradient respectively W_{ij}^c is the polar spin, $\dot{\omega}_i^c$ the rate of Cosserat rotation and e_{ijk} is the permutation tensor.

The proposed hypoplastic Cosserat model includes three state variables, *i.e.* the stress tensor σ, the couple stress tensor μ and the void ratio e. The evolution of the components of these state variables is described by the following equations:

$$\mathring{\sigma}_{ij} = f_s\left[\hat{a}^2 D^c_{ij} + \left(\hat{\sigma}_{kl} D^c_{kl} + \hat{\mu}_{kl}\dot{\kappa}_{kl}\right)\hat{\sigma}_{ij} + f_d\,\hat{a}\left(\hat{\sigma}_{ij} + \hat{\sigma}^*_{ij}\right)\sqrt{D^c_{kl} D^c_{kl} + \dot{\bar{\kappa}}_{kl}\dot{\bar{\kappa}}_{kl}}\right], \tag{1}$$

$$\mathring{\mu}_{ij} = d_{50} f_s\left[a_c^2\dot{\bar{\kappa}}_{ij} + \hat{\mu}_{ij}\left(\hat{\sigma}_{kl} D^c_{kl} + \hat{\mu}_{kl}\dot{\kappa}_{kl} + 2 f_d\, a_c\sqrt{D^c_{kl} D^c_{kl} + \dot{\bar{\kappa}}_{kl}\dot{\bar{\kappa}}_{kl}}\right)\right], \tag{2}$$

$$\dot{e} = (1+e) D_{kk}\ , \tag{3}$$

with the abbreviations:

$$\hat{\sigma}_{ij} = \sigma_{ij}/\sigma_{kk},\quad \hat{\sigma}^*_{ij} = \hat{\sigma}_{ij} - \delta_{ij}/3,\quad \hat{\mu}_{ij} = \mu_{ij}/\left(d_{50}\sigma_{kk}\right)\ \text{ and }\ \dot{\bar{\kappa}}_{ij} = d_{50}\dot{\kappa}_{ij}\,.$$

Herein the objectives stress rate $\mathring{\sigma}$ and objective couple stress rate $\mathring{\mu}$ is rlated to the Jaumann derivative, *i.e.*:

$$\mathring{\sigma}_{ij} = \dot{\sigma}_{ij} - W_{ik}\sigma_{kj} + \sigma_{ik}W_{kj},\quad \mathring{\mu}_{ij} = \dot{\mu}_{ij} - W_{ik}\mu_{kj} + \mu_{ik}W_{kj}.$$

The mean grain diameter d_{50} enters the constitutive equations as the internal length and δ_{ij} denotes the Kronecker delta. The tensor-valued functions of the objective stress rate $\mathring{\sigma}_{ij}$ in Equation (1) and the objective couple stress rate $\mathring{\mu}_{ij}$ in Equation (2) are non-linear in the rate of deformation and the rate of the curvature. Equation (3) implies the assumption that the volume change of the grains can be neglected. Thus, the rate of the void ratio is proportional to the volume strain rate D_{kk}. Factor $\hat{a}$ in Equation (1) and factor a_c in Equation (2) are related to stationary states which can be reached asymptotically under large shearing. In a stationary state the stress ratio becomes higher for a higher $\hat{a}$. Factor $\hat{a}$ depends on the so-called angle of internal friction φ_c, and on the tensor $\hat{\sigma}^{*s}_{kl}$, which represents the symmetric part of the normalised stress deviator, *i.e.* $\hat{\sigma}^{*s}_{kl} = \left(\hat{\sigma}^*_{kl} + \hat{\sigma}^*_{lk}\right)/2$. The proposed function for $\hat{a}$ reads:

$$\hat{a} = \frac{\sin\varphi_c}{3-\sin\varphi_c}\left[\sqrt{\frac{8/3 - 3\left(\hat{\sigma}^{*s}_{kl}\,\hat{\sigma}^{*s}_{kl} + \hat{\sigma}^{*s}_{kl}\,\hat{\sigma}^{*s}_{lm}\,\hat{\sigma}^{*s}_{mk}\right)}{1 - 3\,\hat{\sigma}^{*s}_{kl}\,\hat{\sigma}^{*s}_{lm}\,\hat{\sigma}^{*s}_{mk}/\left(\hat{\sigma}^{*s}_{kl}\,\hat{\sigma}^{*s}_{kl}\right)}} - \sqrt{\hat{\sigma}^{*s}_{kl}\,\hat{\sigma}^{*s}_{kl}}\right]. \tag{4}$$

$\hat{a}$ is embedded in the constitutive Equation (1) and therefore always effective, *e.g.* for isotropic state ($\hat{\sigma}^* = 0$) a value of:

$$\hat{a} = \sqrt{\frac{8}{3}}\,\frac{\sin\varphi_c}{3-\sin\varphi_c}$$

is obtained. The influence of the mean pressure and the current void ratio on the response of the constitutive Equations (1) and (2) is taken into account with the

stiffness factor f_s and the density factor f_d. The evolution of dilatancy, the peak stress ratio, strain softening and the shear zone thickness mainly depend on the density factor f_d, which represents a relation between the current void ratio e, the critical void ratio e_c and the minimum void ratio e_d, *i.e.*:

$$f_d = \left(\frac{e - e_d}{e_c - e_d} \right)^{\alpha}, \tag{5}$$

where $\alpha < 0.5$ is a constitutive constant. The stiffness factor f_s is proportional to the parameter h_s and depends on the stress level σ_{kk} and on the void ratio e, which is related to the maximum void ratio e_i, *i.e.*:

$$f_s = \left(\frac{e_i}{e} \right)^{\beta} \frac{h_s}{n h_i \left(\hat{\sigma}_{kl} \hat{\sigma}_{kl} \right)} \frac{\left(1 + e_i\right)}{e_i} \left(-\frac{\sigma_{kk}}{h_s} \right)^{1-n}, \tag{6}$$

with

$$h_i = \frac{8 \sin^2 \varphi_c}{\left(3 - \sin \varphi_c\right)^2} + 1 - \frac{2\sqrt{2} \sin \varphi_c}{3 - \sin \varphi_c} \left(\frac{e_{i0} - e_{d0}}{e_{c0} - e_{d0}} \right)^{\alpha}.$$

Herein $\beta \geq 1$ is a constitutive constant and the maximum void ratio e_i, is assumed to decrease with the mean pressure σ_{kk} according to the compression relation (Bauer 1995):

$$e_i = e_{i0} \exp\left[-\left(\sigma_{kk} / h_s \right)^n \right]. \tag{7}$$

Herein the constants e_{i0}, h_s and n are related to an isotropic compression test starting from the loosest state of the grain material. It was postulated by Gudehus (1996) that e_c and e_d in Equation (5) decrease with the mean pressure like e_i, *i.e.*:

$$\frac{e_c}{e_{c0}} = \frac{e_d}{e_{d0}} = \frac{e_i}{e_{i0}}, \tag{8}$$

where e_{i0}, e_{c0} and e_{d0} denote the values of e_i, e_c, and e_d for $\sigma_{kk} = 0$.

Altogether the constitutive model includes 11 constants which are closely related to granular properties, *i.e.* they can be estimated from the grain size distribution, the grain shape and grain hardness (*e.g.* Herle and Gudehus 1999). For the present numerical investigations the following material constants are used:

$$e_{i0} = 1.2, \quad e_{d0} = 0.51, \quad e_{c0} = 0.82, \quad \varphi_c = 30°, \quad h_s = 190\text{MPa},$$

$$\alpha = 0.11, \quad \beta = 1.05, \quad n = 0.4, \quad d_{50} = 0.5 \text{ mm}, \quad a_c = 1.0.$$

It can be noted that for purely coaxial homogeneous deformations starting from an initially symmetric stress tensor or for $d_{50} \to 0$ there are no polar effects, *i.e.* $m_{ij} = \dot{m}_{ij} = 0$, $W_{ij} = W_{ij}^c$, $\sigma_{ij}^{*s} = \sigma_{ji}^*$ and $\sigma_{ij} = \sigma_{ji}$, so that the polar hypoplastic model reduces to the non-polar one given by Gudehus (1996) and Bauer (1996), *i.e.*:

$$\overset{\circ}{\sigma}_{ij} = f_s\left[\hat{a}^2 D_{ij} + \hat{\sigma}_{ij}\left(\hat{\sigma}_{kl} D_{kl}\right) + f_d \hat{a}\left(\hat{\sigma}_{ij} + \hat{\sigma}^*_{ij}\right)\sqrt{D_{kl} D_{kl}}\right],$$

$$\dot{e} = (1+e) D_{kk}.$$

3. Modelling of the interface behaviour

Besides the stress and displacement boundary conditions of a non-polar continuum additional non-standard boundary conditions, *i.e.* couple stresses and Cosserat rotation boundary conditions, must also be taken into account. Along the walls of bounding structures in motion the slide and rotation resistance of the particles in contact is mainly determined by the interaction between the wall roughness and the size, shape and roughness of the grains. Very rough walls can capture the adjoining small grains so that neither sliding nor rotating may occur. Then the relative displacement and the Cosserat rotation at the boundary of the granular body is zero. For rough and medium rough boundaries and quasi-static processes the following assumptions are made to model the interface behaviour in a simplified manner:

i) Boundary particles of the granular body are permanently in contact with the adjoining structure. Therefore the relative displacement $u_{r\perp}$ of the particles perpendicular to the adjoining structure surface is zero, *i.e.*:

$$u_{r\perp} = 0. \tag{9}$$

ii) The tangential displacement $u_{p\|}$ of the particles along the surface of the adjoining structure is equal to or less than the displacements of the adjoining structure $u_{s\|}$, *i.e.*:

$$u_{p\|} = f_u u_{s\|}. \tag{10}$$

Herein the dimensionless factor $0 \le f_u \le 1$ denotes the fraction of $u_{s\|}$ which is transmitted to the boundary of the granular body. Then the relative displacement $u_{r\|}$ between the boundary surfaces reads:

$$u_{r\|} = u_{s\|} - u_{p\|} = (1 - f_u) u_{s\|}. \tag{11}$$

iii) The cosserat rotation ω_p^c at the boundary of the granular body can be related to the displacement $u_{s\|}$ according to the relation proposed by Tejchman (1997), *i.e.*:

$$\omega_p^c = f_\omega \frac{u_{s\|}}{d_{50}}, \tag{12}$$

where the dimensionless factor f_ω denotes the fraction of $u_{s\|}$ which is transmitted as rotation. For the special case of pure rolling the relative

displacement is $u_{r\|} = \omega_p^c \, d_{50}/2 = u_{s\|}/2$, factor f_u becomes 1/2 and an upper limit of $f_\omega = 1$ can be derived.

With respect to relations (10) and (11) ω_p^c can alternatively be represented as a function of the boundary displacement $u_{p\|}$ of the granular layer, *i.e.:*

$$\omega_p^c = \frac{f_\omega}{f_u} \frac{u_{p\|}}{d_{50}}, \tag{13}$$

or as a function of the relative displacement $u_{r\|}$, *i.e.*:

$$\omega_p^c = \frac{f_\omega}{1 - f_u} \frac{u_{r\|}}{d_{50}}. \tag{14}$$

4. Finite element analysis of plane shearing

For numerical simulations of plane shearing the present hypoplastic Cosserat model was implemented in the finite element code ABAQUS (5.8-1) using the user-element interface UEL. A four-node element with bilinear shape functions was used to describe the displacements and Cosserat rotations within the element. For the case of plane strain only three degrees of freedom remain for each node, *i.e.* u_1, u_2 and ω_3^c, as shown in Figure 1. A so-called selective reduced integration technique was adopted to alleviate volumetric locking (Nagtegaal, Parks and Rice 1974). A Newton iteration procedure is used to solve the non-linear equation system and an implicit time integration technique is applied to compute the stress and couple stress increments. Since the material behaviour to be described is rate-independent the time increment can, for instance, be related to the increment of the initiated shear displacement.

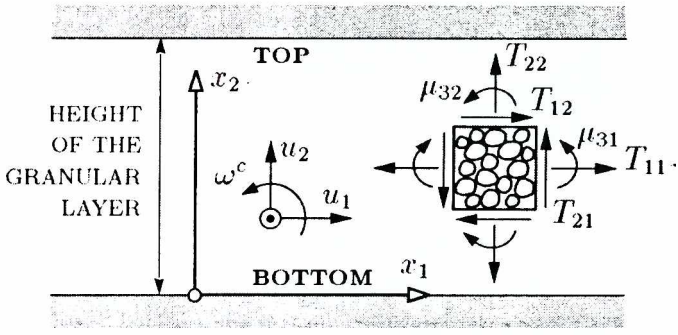

Figure 1. *Modelling a plane shear layer of granular material with a Cosserat continuum (displacements u_i, Cosserat rotation ω_3^c, stresses σ_{ij} and couple stresses μ_{ij})*

4.1 Influence of the lateral boundary conditions

The distribution of the deformation and void ratio within a shear specimen is shown in Figure 2 for different boundary conditions described at the lateral boundaries of the specimen. All calculations are carried out under plane strain conditions starting from an initially homogeneous isotropic state with $e_o = 0.6$, $\sigma_o = -100$ kPa and $m_o = 0$. At the top boundary the vertical stress σ_{22} is kept constant and a shear displacement is initiated by prescribed horizontal node displacemets, while the vertical displacement is obtained as a result of dilatancy behaviour within the whole specimen. The node displacements are locked at the bottom and the rotation degrees of freedom are locked for both bottom nodes and top nodes.

In order to model the lateral boundary conditions of the classical plane simple shear test a linear displacement field must be prescribed on both sides of the

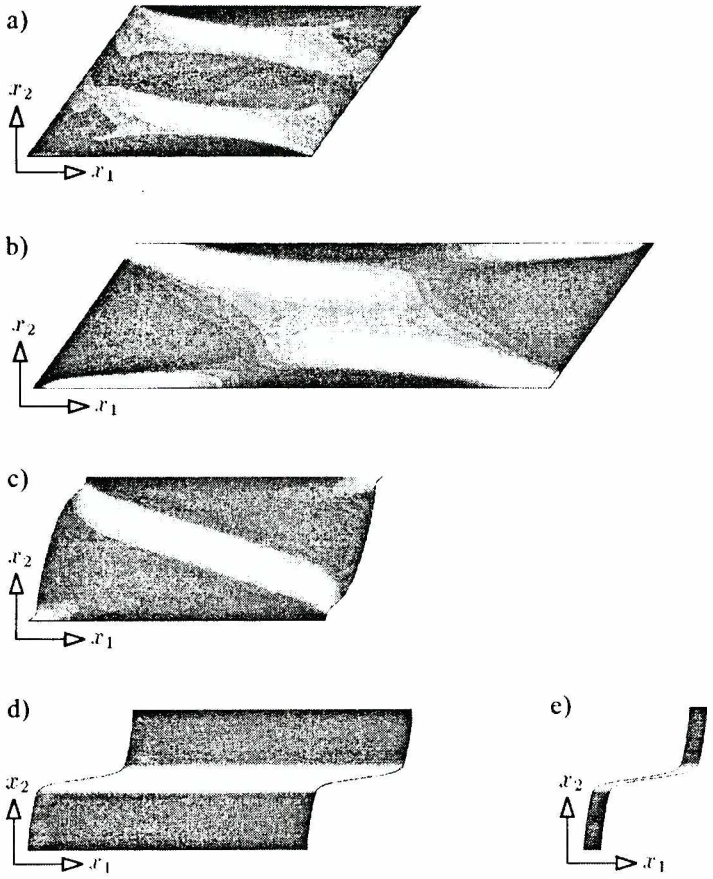

Figure 2. *Influence of prescribed lateral boundary conditions on the distribution of the void ratio within a shear layer for: (a) and (b) lateral linear displacement fields; (c) lateral constant pressures; (d) and (e) symmetric conditions of an infinite shear layer*

specimen (Figures 2a and 2b). The numerical investigation shows that in contrast to a classical continuum the distribution of the state quantities within the specimen obtained for a polar continuum becomes strongly heterogeneous from the beginning of shearing. The brighter bands indicate a higher void ratio and consequently the location where failure starts. The zones are eccentrically located and slightly inclined, which also reflects the experimental observation made with the so-called simple shear apparatus of the Cambridge type on sand specimens (Rosce 1973). The distribution of the void ratio changes with the horizontal co-ordinate and it is also influenced by the length of the specimen as can clearly be seen by comparing Figure 2a with Figure 2b. For shearing under a constant lateral pressure the deformation field is also rather heterogeneous as shown in Figure 2c. It is obvious that the lateral boundary conditions assumed in Figures 2a, 2b, 2c have a significant influence on the evolution of the state quantity, *i.e.* the quantities change with the horizontal co-ordinate and their distribution is influenced by the geometrical dimension of the specimen. The results are independent of the horizontal co-ordinate (Figure 2d) if the symmetry conditions for an infinite shear layer are introduced (Bauer and Huang 1999). The symmetry condition can be modelled by applying constraint conditions to the side nodes of the finite element mesh, *i.e.* each node on the left boundary is controlled to have the same displacements and Cosserat rotation as the corresponding node with the same vertical co-ordinate on the right boundary. Thus, for a finite element calculation of an infinite shear layer a single column of elements is sufficient (Figure 2e).

4.2 Behaviour of an infinite shear layer

In the following the influence of the Cosserat boundary conditions at the top surface of an infinite shear layer is discussed. All the finite element calculations are performed for a shear layer with a height of 4 cm starting from the same homogeneous and isotropic initial states as described in Section 4.1. The kinematical boundary conditions at the bottom are $u_{1_B} = u_{2_B} = 0$ and $\omega^c_{3_B} = 0$. At the top surface the vertical pressure of $\sigma_{22} = -100$ kPa is kept constant and the horizontal displacement u_{i_T} and the Cosserat rotation $\omega^c_{3_T} = -f_B u_{1_T}/d_{50}$ are described.

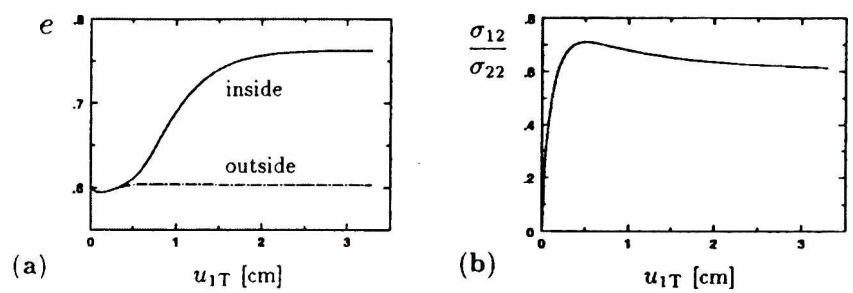

Figure 3. *Plane shearing of an infinite layer: (a) void ratio inside and outside of the localisation zone; (b) stress ratio at the top surface versus shear displacement* u_{1_T}

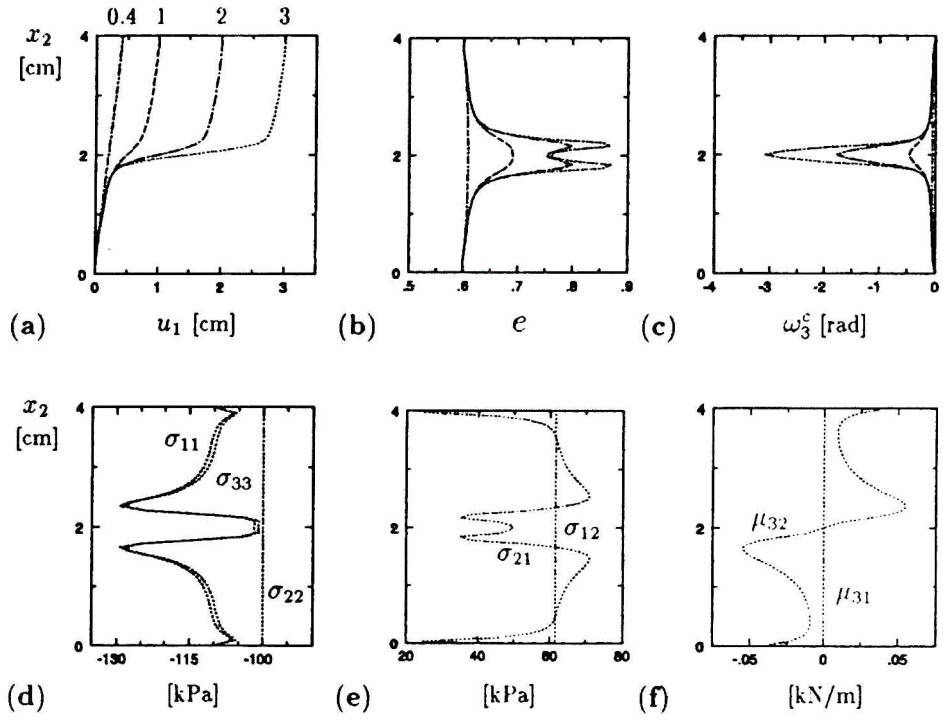

Figure 4. *Plane shearing between two very rough surfaces under a constant vertical pressure of* $\sigma_{22} = -100$ *kPa: (a) horizontal displacements* u_1, *(b) void ratio e, and (c) Cosserat rotation* ω_3^c *across the height of the layer for shear deformation of* $u_{1_T} = 0.4, 1, 2, 3$ *cm; (d) normal stresses, (e) shear stresses, and (f) couple stresses for a shear deformation at the top boundary of* $u_{1_T} = 3$ *cm*

For symmetric Cosserat boundary conditions, *i.e.* locked Cosserat rotations at the bottom and top surfaces, the deformation for large shearing is localised within a narrow zone in the middle of the layer (Figure 2d). The light strip indicates a higher void ratio as a result of dilatancy within the localised zone. Figure 3a shows the evolution of the void ratio in an element inside and outside of the localised zone. At the beginning of shearing the void ratio slightly decreases and then increases, which means that the material first becomes denser and shows dilatancy with advanced deformation. However, before the stress peak is reached the void ratio curves branch out. The void ratio inside the localised zone increases very strongly and tends towards a stationary value while the void ratio outside the localised zone slightly increases and becomes almost constant for continuous shearing. This indicates that for a continuous shearing the material outside the localised zone behaves like a rigid body after the stress peak. The horizontal shear resistance versus the horizontal displacement at the top is shown in Figure 3b. First the shear resistance increases up to a peak state and afterwards the value decreases and tends towards a stationary state.

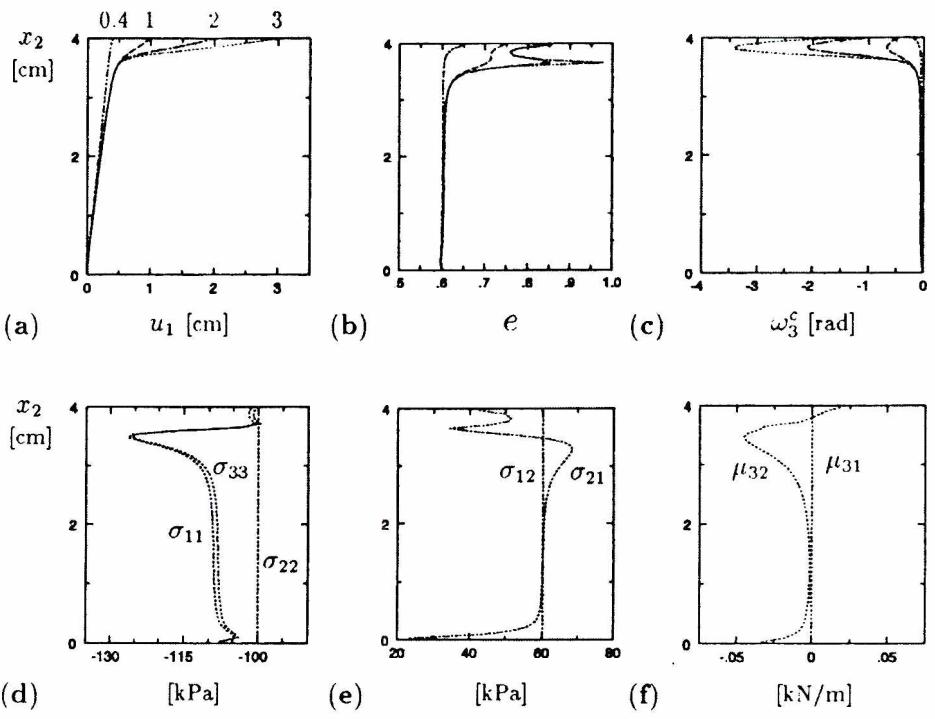

Figure 5. *Plane shearing between a very rough bottom and a medium rough top surface under a constant vertical pressure of $\sigma_{22} = -100$ kPa: (a) horizontal displacements u_1, (b) void ratio e and (c) Cosserat rotation ω_3^c across the height of the layer for shear deformation of $u_{1T} = 0.4, 1, 2, 3$ cm; (d) normal stresses, (e) shear stresses, and (f) couple stresses for a shear deformation at the top boundary of $u_{1T} = 3$ cm*

For a shear displacement of 0.4, 1, 2 and 3 cm at the top of the layer the distribution of the horizontal displacements u_1, the void ratio e and the Cosserat rotations ω_3^c across the height of the layer are shown in Figures 4a, 4b and 4c. It can clearly be seen that the void ratio e and the Cosserat rotation ω_3^c increases within the localised zone, while outside this zone these quantities remain almost unchanged. The distribution of the stress components σ_{11} and σ_{21} is influenced by polar effect while σ_{22} and σ_{12} are constant as it is required for the equilibrium (Figure 4d and Figure 4e). Since $\sigma_{12} \neq \sigma_{21}$ the stress tensor in the frame of a polar continuum is nonsymmetric. It can be pointed out that the couple stress μ_{31} is very small (Figure 4f), but it does not vanish across the shear layer due to the contribution of the Jaumann terms.

For different Cosserat boundary conditions at the bottom and at the top boundaries the zone of strain localisation is no longer located in the middle of the shear layer. The results in Figure 5 were found for a smoother top surface which was modelled by prescribing the Cosserat rotation at the top boundary using relation (13) with

$\omega^c_{3T} = -0.025\ u_{1T}/d_{50}$. It is obvious that the zone of strain localisation is located near the smoother boundary and the distribution of the state quantities is different to the results obtained for symmetric Cosserat boundary conditions. Furthermore, the thickness of the localised zone is smaller than the value found for the symmetric case. Independent of the assumed boundary condition for ω^c_{3T} the normal stresses and the void ratio in the middle of the localised zone tend towards the same stationary value that is obtained from the non-polar hypoplastic model under plane shearing (Bauer 2000), *i.e.* the state quantities tend towards $T_{11} = T_{22} = T_{33}$ and $e = e_c$. At the boundary of the localised zone the stresses and couple stresses are extremal and the void ratio in this zone becomes greater than the critical one. Thus, an initially isotropic material gets a transversely isotropic structure during shearing.

4.3 Influence of the initial state quantities on the thickness of the localised zone

For symmetric Cosserat boundary conditions *i.e.* $\omega^c_{3B} = \omega^c_{3T} = 0$, the influence of the initial state on the thickness of localised zone is shown in Figure 6. The results for different vertical pressures (Figure 6a) and initial void ratios (Figure 6b) indicates that the thickness t of the localised zone increases with an increase of the pressure σ_{22}, the initial void ratio e_o and the mean grain diameter d_{50}. For non-symmetric

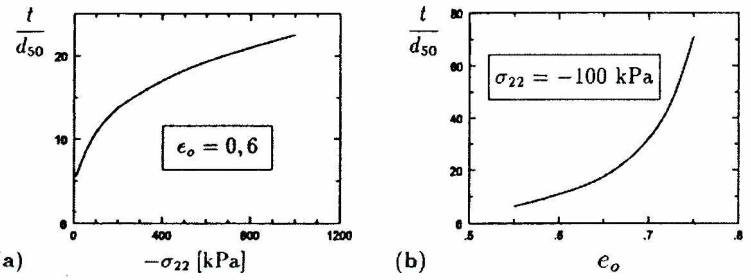

Figure 6. *Influence of the initial state on the thickness t of the localised zone: (a) t/d_{50} versus vertical pressure σ_{22} for $e_o = 0.6$; (b) t/d_{50} versus initial void ratio e_o for $\sigma_{22} = -100$ kPa*

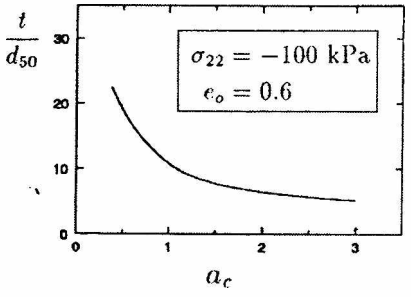

Figure 7. *Influence of the polar constant a_c on the shear band thickness*

Cosserat boundary conditions the thickness of the localised zone is smaller, as was already mentioned in Section 4.2. The foregoing investigations were carried out for $a_c = 1.0$. The polar constant a_c in the evolution Equation (2) for the couple stresses takes into account the influence of the grain shape and grain roughness on the rotation resistance of particles. The investigations show that a_c influences the shear band thickness and it is directly related to the Cosserat quantities in a stationary state. The thickness of the shear band decreases with an increase of a_c (Figure 7).

5. Conclusion

Polar effects resulting from grain rotation and couple stresses in a granular material can be accounted for with the presented polar hypoplastic model. Finite element calculations were performed to study the response of an infinite layer of granular material under plane shearing. Proper constraints were used to model the symmetry conditions of an infinite layer with respect to a polar continuum. From the numerical investigations it follows that polar effects within shear zones are noticeable. Their influence on the evolution of the current stress and void ratio is significant. For large shearing the deformation is localised within a narrow zone. The thickness of the zone is higher for an initially higher void ratio and is also influenced by the roughness of the boundaries, the mean grain diameter and the pressure level. For symmetric boundary conditions at the top and at the bottom of the shear layer the localised zone occurs in the middle of the shear layer, otherwise it is located near the smoother boundary.

References

[1] Bauer E. and Tejchman J., *Numerical study of the effect of grain rotations on material behaviour in a fault zone*, Proc. of the 2th Int. Conf. on the Mechanics of Jointed and Faulted Rock, ed. Rossmanith, Balkema, 1995, 317, 1995

[2] Bauer E., *Calibration of a comprehensive hypoplastic model for granular materials*, Soils and Foundations, **36**, 13, 1996

[3] Bauer E. and Huang W., *Numerical investigation of polar effects in a Cosserat material under shearing*, Proc. of the Int. Workshop on Fracture Mechanics and Advanced Engineering Materials, Sydney, Australia, University of Sydney, 311, 1999

[4] Bauer E., *Conditions for embedding Casagrande's critical states into hypoplasticity*, Mechanics of Cohesive-Frictional Materials, No. 5, 125, 2000

[5] Bogdanova-Bontcheva N. and Lippmann H., *Rotationssymmetrisches ebenes Fliessen eines granularen*, Modellmaterials Acta Mechanica, **21**, 93, 1975

[6] de Borst R., Mühlhaus H. B., Pamin J. and Sluys L.Y., *Computational modelling of localisation of deformation*, Proc. 3th Int. Conf. Comp. Plast, Pineridge Press, Swansea, 483, 1992

[7] Gudehus G., *Localisation in granular bodies — Position and objectives*, Proc. of the 3th Int. Workshop on Localisation and Bifurcation Theory for Soils and Rocks, eds. Chambon, Desrues and Vardoulakis, Balkema, 1994, 3, 1993

[8] Gudehus G., *A comprehensive constitutive equation for granular materials*, Soils and Foundations, **36**, 1, 1996

[9] Gudehus G., *Attractors, percolation thresholds and phase limits of granular soils*, Powders and grains, eds. Behringer and Jenkins, Balkema, 169, 1997

[10] Gudehus G., *Shear localisation in simple grain skeleton with polar effect*, Proc. of the 4th Int. Workshop on Localisation and Bifurcation Theory for Soils and Rocks, eds. Adachi, Oka and Yashima, Balkema, 1998, 3, 1997

[11] Herle I. and Tejchman J., *Effects of grain size and pressure level on bearing capacity of footings on sand*, Deformation and Progressive Failure in Geomechanics, eds. Asaoka, Adachi and Oka, Elsevier Science, 781, 1997

[12] Herle I. and Gudehus G., *Determination of parameters of a hypoplastic constitutive model from properties of grain assemblies*, Mechanics of Cohesive-Frictional materials, **4**, 461, 1999

[13] Mühlhaus H. B., *Shear band analysis in granular materials by Cosserat theory*, Ing. Arch., **56**, 271, 1986

[14] Mühlhaus H. B. and Vardoulakis I. , *The thickness of shear bands in granular materials*, Géotechnique, **37**, 271, 1987

[15] Nagtegaal J. C., Parks D. M. and Rice J. R., *On numerically accurate finite element solutions in the fully plastic range*, Comp. Meth. Appl. Mech. Engng., **4**, 153, 1974

[16] Oda M., *Micro-fabric and couple stress in shear bands of granular materials*, Powders and Grains, ed. C. Thornton, **3**, 161, 1993

[17] Oda M., Iwashita K. and Kazama H., *Micro-structure developed in shear bands of dense granular soils and its computer simulation — Mechanism of dilatancy and failure*, In IUTAM Symposium on Mechanics of Granular and Porous Materials, Cambridge, U.K., eds. Fleck Cocks, 353, 1996

[18] Oda M., Tatsuoka F. and Yoshida T., *Void ratio in shear band of dense granular soils*, Deformation and Progressive Failure in Geomechnaics, eds. Asaoka, Adachi and Oka, Pergamon, 157, 1997

[19] Roscoe K. H., *The influence of strains in soil mechanics*, 10th Rankine Lecture. Géotechnique, **20**, 129, 1970

[20] Tejchman J., *Scherzonenbildung und Verspannungseffekte in Granulaten unter Berücksichtigung von Korndrehungen*, Veröffentlichungen des Institutes für Bodenmechanik und Felsmechanik der Universität Fridericiana in Karlsruhe, **117**, 1989

[21] Tejchman J. and Bauer E., *Numerical simulation of shear band formation with a polar hypoplastic constitutive model*, Computers and Geotechnics, **19**, 221, 1996

[22] Tejchman J., *Numerical modelling of shear localisation with a polar hypoplastic approach*, Proc. of the 4th Int. Workshop on Localisation and Bifurcation Theory for Soils and Rocks, eds. Adachi, Oka and Yashima, Balkema, 1996, **323**, 1998

[23] Tejchman J., *Modelling of shear localisation and autogeneous dynamic effects in granular bodies*, Veröffentlichungen des Institutes für Bodenmechanik und Felsmechanik der Universität Fridericiana in Karlsruhe, **140**, 1997

[24] Tejchman J. and Gudehus G., *Shearing of a narrow granular layer with polar quantities*, Submitted to Int. J. Num. Anal. Meth. Geomech, 1999

[25] Uesugi M., Kishida H. and Tsubakihara Y., *Behaviour of sand particles in sand-steel friction*, Soils and Foundations, **28**, 107, 1998

[26] Vardoulakis I. and Sulem J., *Bifurcation Analysis in Geomechanics*, Blackie Academic & Professional, London, 1995

[27] Wehr W., Tejchman J., Herle I. and Gudehus G., *Sand anchors — a shear zone problem*, Deformation and Progressive Failure in Geomechanics, eds. Asaoka, Adachi and Oka, Elsevier Science, 787, 1997